

Amorphous Photonic Lattices: Band Gaps, Effective Mass, and Suppressed Transport

Mikael Rechtsman,¹ Alexander Szameit,¹ Felix Dreisow,² Matthias Heinrich,² Robert Keil,² Stefan Nolte,² and Mordechai Segev¹

¹*Physics Department and Solid State Institute, Technion, 32000 Haifa, Israel*

²*Institute of Applied Physics, Friedrich-Schiller-Universität Jena, Max-Wien-Platz 1, 07743 Jena, Germany*
(Received 12 October 2010; revised manuscript received 13 February 2011; published 13 May 2011)

We study, experimentally and numerically, amorphous photonic lattices and the existence of band gaps therein. Our amorphous system comprises 2D waveguides distributed randomly according to a liquidlike model responsible for the absence of Bragg peaks, as opposed to ordered lattices with disorder which always exhibit Bragg peaks. In amorphous lattices the bands comprise localized states, but we find that defect states residing in the gap are more localized than the localization length of states within the band. Finally, we show how the concept of effective mass carries over to amorphous photonic lattices.

DOI: 10.1103/PhysRevLett.106.193904

PACS numbers: 42.82.Et, 42.25.Dd, 42.25.Fx, 61.43.Dg

Conventional intuition holds that, for a solid to have an electronic band gap, it must be periodic, allowing the use of Bloch's theorem. Indeed, the free-electron approximation implies that Bragg scattering in periodic potentials is a precondition for the formation of a band gap. But this is untrue: looking through a window reveals that glassy silica, although possessing no long-range order, still displays an electronic band gap spanning the spectrum of visible light, which is responsible for the lack of absorption. Amorphous band gaps were explored theoretically in 1971 [1], and experiments in electronic systems followed [2,3]. With the major progress in photonic crystals [4], it is natural to explore amorphous photonic media. Indeed, these were studied theoretically [5–7], and microwave experiments demonstrated the existence of a band gap [5]. However, amorphous band-gap media have never been studied experimentally in the optical regime.

Here, we present the first experiments of amorphous photonic lattices in the optical regime exhibiting a band gap: a liquidlike two-dimensional (2D) array of randomly organized evanescently coupled waveguides. We show that the bands in this medium are separated by gaps in its spatial spectrum, despite lack of Bragg scattering. The liquidlike distribution plays a key role in the absence of Bragg peaks, because in a periodic lattice containing disorder, Bragg peaks are always present. The bands in amorphous photonic media are comprised of inherently localized Anderson states, yet we find that these lattices support strongly localized defect states, whose widths are much narrower than the Anderson localization lengths of states well within the band. Finally, we show the existence of a region of negative effective mass (anomalous diffraction) [8], and how to observe it in transport experiments. Amorphous photonic lattices are a test bed for the properties of general amorphous systems, because optics allows us to precisely engineer the potential, as well as to employ nonlinearity under controlled conditions. Hence, this work paves the way for unraveling features that are much harder to access experimentally in other systems.

The evolution of the optical wave $\Psi(x, y, z)$ in our paraxial system is described by

$$i\lambda \frac{\partial \Psi(x, y, z)}{\partial z} = - \left[\frac{\lambda^2}{2n_0} \nabla_{\perp}^2 + \Delta n(x, y) \right] \Psi(x, y, z) \quad (1)$$

where $\lambda = \lambda/2\pi$ is the reduced wavelength, n_0 is the refractive index of the bulk, and $\Delta n(x, y)$ is the n_0 modulation caused by the random distribution of identical waveguides. Equation (1) is similar to the Schrödinger equation, when λ is replaced by \hbar , n_0 by the mass m , $\Delta n(x, y)$ by the potential $-V(x, y)$, and the spatial coordinate z by time t [9]. This similarity was used in many experiments, demonstrating concepts from solid-state physics using optical settings [9]. One important example is Anderson localization, which was realized in photonic lattices [10] using the transverse localization scheme [11]. To obtain the band structure, one needs to solve Eq. (1), by substituting $\Psi(x, y, z) = \varphi(x, y)e^{i\beta z}$ with the propagation constant β . Here, the resulting eigenvalue equation cannot be solved by applying Bloch's theorem, since $\Delta n(x, y)$ is not periodic (further discussion in section A of EPAPS [12]). Rather, as known from Anderson localization in 2D, the eigenmodes are fully localized ("Anderson states"). Consequently, one must solve using the full refractive index profile to find the eigenvalue spectrum.

Our liquidlike amorphous lattices have no long-range order, and lack any diffraction peaks. We distribute the waveguides as a snapshot of atoms in a liquid by the use of the Metropolis Monte Carlo method with a repulsive interatomic force [13] (further discussion in section B of EPAPS [12]). Such structures result in random $\Delta n(x, y)$, with one particular realization shown in Fig. 1(a). The modulus of the Fourier transform of $\Delta n(x, y)$ has no delta-function peaks [Fig. 1(b)]. The broad elliptic rings are similar to those seen in x-ray scattering on liquids. Figure 1(c) shows a disordered pattern where the position of each waveguide is randomly and independently perturbed, from a square lattice. In sharp contrast to the amorphous case, the modulus of the Fourier transform of

this pattern displays pronounced Bragg peaks [Fig. 1(d)]. The presence of long-range order in the perturbed crystal always gives rise to Bragg scattering, exemplifying the fundamental difference between amorphous media and a crystal containing disorder.

We fabricate a waveguide array corresponding to the structure of Figs. 1(a) and 1(b) using direct laser writing [14] (further discussion in section C of EPAPS [12]). Figure 2(a) depicts an image of the structure. All waveguides have identical structure (slightly elliptic, due to fabrication constraints), and the refractive index step defining them is $\Delta n = 9 \times 10^{-4}$. As Fig. 2(b) shows, the Fourier transform of this amorphous structure displays a total lack of Bragg peaks. We calculate the eigenmodes of this structure, and show in Fig. 2(c) the values of β for $\lambda = 633$ nm. The values of β for this structure at $\lambda = 633$ nm are shown in Fig. 2(c). Figure 2(c) reveals a sizeable gap in the spatial spectrum, despite a total lack of periodicity (and lack of Bragg scattering) in Fig. 2(b). This defies a common argument [15], stating that gaps open at the boundary of the Brillouin zone because the degeneracy of states there is broken by the periodicity of the potential.

A nice feature offered by optical settings described by Eq. (1) is the ability to test the properties of the system by tuning parameters independently. The most notable one is λ , which can be tuned continuously. The inset in Fig. 2(c) reveals that the gap width is exponentially decreasing with λ (when all other parameters are fixed), until it closes at 900 nm. This can be understood from Eq. (1): increasing λ leads to a larger “kinetic energy” (∇_T^2), and thus to relative weakening of the potential inducing the gap.

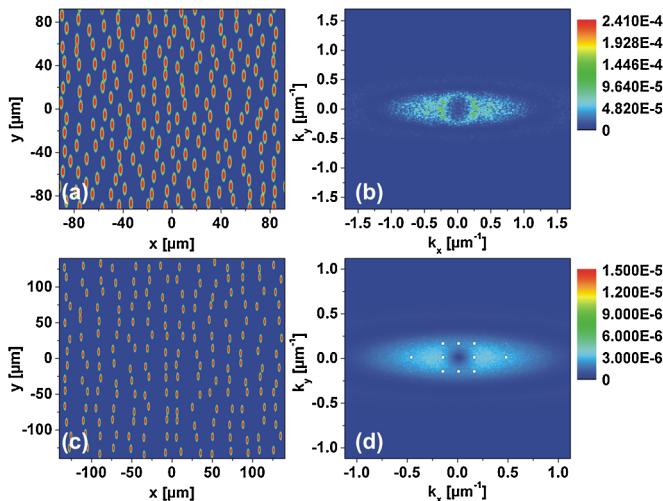


FIG. 1 (color online). Theoretical results. (a) Refractive index profile, $n(x, y)$, of an amorphous waveguide structure. The index varies from 1.45 to $1.45 + 9 \times 10^{-4}$. (b) Modulus of the Fourier transform of this structure, which shows no Bragg peaks. (c) $n(x, y)$ for a square lattice with superimposed uncorrelated disorder. (d) Modulus of the Fourier transform of (c), displaying clear Bragg peaks. Note that (b) and (d) were averaged over many different realizations to highlight the Bragg peaks.

The band gap in amorphous systems calls for some intuition. In the structure of Figs. 1 and 2, all waveguides are identical, but their spacing is random. It is instructive to plot the size of the gap as a function of the variance of the interwaveguide spacing (variance in the tight-binding hopping parameter). We plot that in Fig. 2(d) for $\lambda = 633$ nm, and find that there is a sizeable gap as long as the normalized standard deviation is below 18%. The key feature of our liquidlike structure giving rise to the large band gap is the short-range order: the waveguides have similar spacing; thus, they form bonds of similar energy and in turn, populate the bands and leave the gap empty. The presence of short-range order is known to give rise to band gaps in amorphous systems [16], whereas the lack of long-range order is responsible for the absence of Bragg peaks.

To visualize the gap experimentally, we introduce a defect waveguide in the structure: a single waveguide with a refractive index maximum lower by $\Delta n_d = 4.5 \times 10^{-4}$ than all other waveguides. Calculations show that this results in a single, negative, defect state residing directly in the band gap [Fig. 3(a)], for $\lambda = 633$ nm. By contrast, at $\lambda = 875$ nm the gap is extremely small; hence, the defect state occurs where the bands merge [Fig. 3(b)]. Consequently, when we launch a $\lambda = 633$ nm beam into the defect waveguide, the beam stays strongly confined throughout propagation, because it excites a highly localized defect state. This is shown experimentally in Fig. 3(c), which depicts the structure of the beam exiting the amorphous lattice. The coupling to all nearby waveguides is greatly suppressed, in spite of their close proximity, as light is guided in a defect state residing in a sizeable band gap. In contrast, at $\lambda = 875$ nm there is no gap; hence, a 875 nm

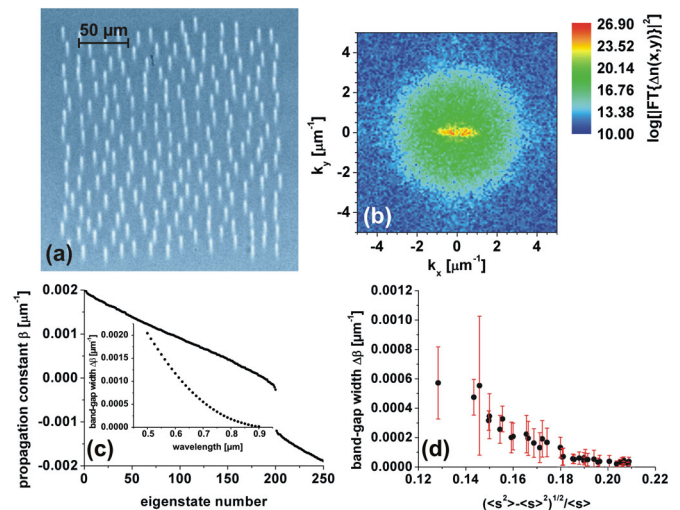


FIG. 2 (color online). Amorphous photonic lattices: experiments. (a) Microscope image of the input facet of the waveguide lattice. (b) Modulus of the Fourier transform of (a), showing no Bragg peaks. (c) Eigenvalue spectrum of the amorphous lattice at $\lambda = 633$ nm, showing a band gap. Inset: size of the band gap as a function of λ . (d) Variation of band gap size as a function of standard deviation of the spacing between waveguides.

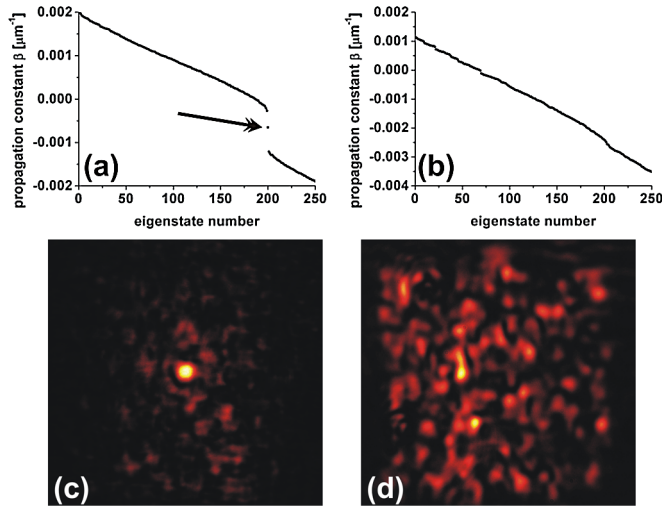


FIG. 3 (color online). (a),(b) Eigenvalue spectrum of the amorphous lattice with a defect waveguide at $\lambda = 633$ nm and $\lambda = 875$ nm: (a) contains a defect mode in its gap (indicated by arrow), while (b) has no gap and therefore no defect mode. (c), (d) Experimental images of the light intensity at output facet, showing a highly localized defect mode in the gap in (c), but not in (d).

beam launched into the same waveguide tunnels to many other waveguides [Fig. 3(d)]. Thus, by demonstrating the presence of the defect state, we show the existence of a band gap in this amorphous optical system.

We now demonstrate that a defect state in our amorphous system is much more localized than a typical Anderson state lying within the band. In infinite 2D systems, all states are inherently localized with any amount of disorder [17]. As we will show, despite the fact that our system size is not sufficiently large to assure that each eigenstate is exponentially localized, when we excite any single nondefect waveguide far from the sample edges (thereby exciting a superposition of modes within the band), the wave packet acquires an exponentially decaying profile after propagation through the sample, a hallmark of Anderson localization. It is therefore interesting to compare Anderson localization in our amorphous lattice with the light confinement in a defect state residing within the gap. This question is of fundamental importance, and has never been addressed experimentally. Figure 4 shows the results: a defect state (residing in the gap) is much more localized than the Anderson localization length of states residing in the bands.

The profile of the defect mode is obtained by imaging the light exiting the defect waveguide. The profile of the Anderson-localized wave packet is obtained similarly. Such experiments on Anderson localization require ensemble averaging over multiple realizations of disorder to obtain meaningful results [10]. Figures 4(a) and 4(b) depict the intensity profile of light trapped in a defect mode [Fig. 4(a)], and light that is Anderson localized [Fig. 4(b)]. The defect state is invariant under averaging, in contrast to a beam made of Anderson modes (which are part of the

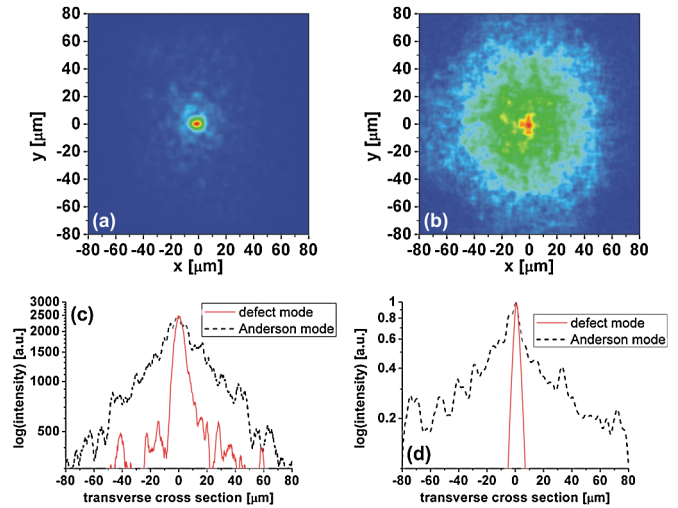


FIG. 4 (color online). (a) Experimental ensemble-averaged output beam for light launched into the defect waveguide. Ensemble averaging does not affect the shape of the defect mode. (b) Experimental ensemble-average output beam for 633 nm light input on 30 different nondefect waveguides in different local environments of the disordered pattern. The ensemble-average wave packet exhibits Anderson localization. (c) Semilog light intensity cross sections for the experiments of (a) and (b). (d) Numerical results for curves corresponding to those in (c) derived from beam-propagation simulations. The defect state is always narrower than the Anderson localization length.

band), where a single realization does not reveal the arrest of transport by disorder. Figures 4(c) and 4(d) show the cross section taken through the experimental [Figs. 4(a) and 4(b)] and simulated results under the experimental conditions. These figures reveal that the defect state is much narrower than the localization length. This is because the defect state exhibits an isolated eigenvalue, with no other states of similar energy with which it may hybridize and thus delocalize. It is similar to more localized states spreading out into the gap from the band edges [18] (which are exceedingly rare due to their low density of states), or doping states in electronic systems [19]. Interestingly, we find that the width of a defect state residing in the gap of our amorphous structure is comparable to that of a defect state in the gap of a fully periodic crystal of the same (mean) lattice spacing.

Next, we show that the concept of *effective mass* at the band edges carries over from the periodic to the amorphous case. The presence of quasiparticles (electrons and holes with positive and negative effective mass) at the Fermi energy in amorphous electronic systems is well established [8]. In photonic lattices, the effective mass is defined as the inverse of the second derivative of the propagation constant with respect to the transverse momentum. Hence, the effective mass in photonic lattices is measured by varying the transverse Bloch momentum of a launch beam and observing the variation of its transverse group velocity [9], assuming the eigenstates are Bloch modes. However, in amorphous systems, Bloch's theorem does not apply,

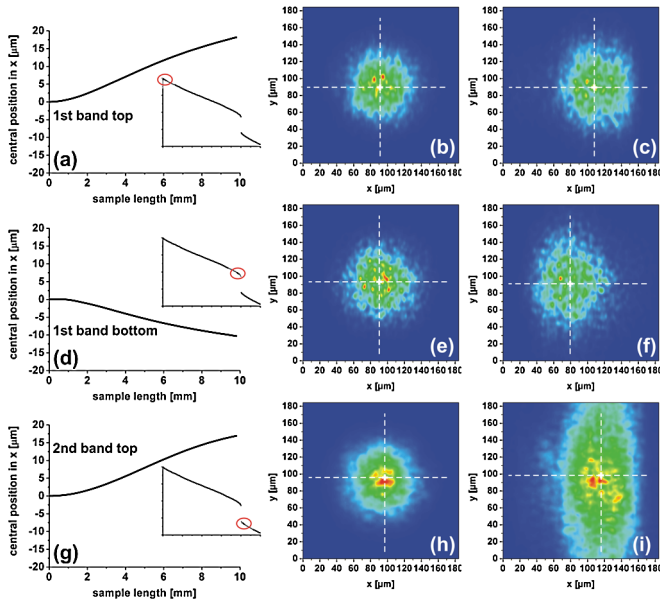


FIG. 5 (color online). Quantifying the effective mass through deflection. Top, middle, bottom rows: deflection of a wave packet taken from the top edge of the first band, bottom edge of first band, and top edge of the second band, respectively. Left, middle, and right column: deflection vs propagation distance, input light distribution, and output light distribution, respectively. The deflections in (c), (f), (k), indicate positive, negative, and positive effective mass, respectively. All results are ensemble averaged over 100 realizations of the amorphous pattern.

so the effective mass is poorly defined. Instead, we quantify the effective mass through Newton's second law: introducing a slow variation of the potential, we launch a wave packet, and observe its trajectory. An example is shown in Fig. 5, where we add a weak, slowly varying, sinusoidal function to the structure $\Delta n(x, y) \rightarrow \Delta n(x, y) + \alpha \sin(2\pi x/L)$, where L is the width of the sample, and $(0,0)$ is taken to be at the center [20]. Then, we construct a beam from a superposition of eigenstates within a small range of β at close vicinity, and launch it near the center coordinate. With $\alpha > 0$ the force acts in the $+x$ direction. Hence, for a positive effective mass, the beam would be deflected towards $+x$, whereas for a negative effective mass it would propagate in the $-x$ direction, opposite to the force. The amount of deflection is inversely proportional to the effective mass. We demonstrate this concept through simulations. Figure 5 demonstrates that at the tops of the first and second bands, the effective mass is positive, and at the bottom of the first band it is negative. Thus, the concept of effective mass carries over to amorphous systems. This suggests interesting experiments, especially in the nonlinear regime—where an attractive nonlinearity would act the opposite for positive and negative effective mass [21], even though the potential is random.

In this Letter, we demonstrated the existence of band gaps in amorphous lattices. This raises many intriguing

questions, such as, how does nonlinearity impact light evolution in such media? Would a repulsive nonlinearity lead to suppression of transport for wave packets with negative effective mass? Would nonlinear phenomena, such as spontaneous pattern formation, exist in amorphous media? Is it possible to generate solitons in amorphous media? If so, then how would solitons move through the random potential and interact with one another? Our setting will help exploring these concepts and understand the true universal nature of amorphous media.

This work was supported by an Advanced Grant from the ERC by the Israel Ministry of Science and by the German-Israel Foundation. M.C.R. is grateful to the Azrieli Foundation for support through an Azrieli Fellowship. A.S. acknowledges support by the Leopoldina-German Academy of Sciences.

- [1] D. Weaire and M.F. Thorpe, *Phys. Rev. B* **4**, 2508 (1971).
- [2] K. Morigaki, *Physics of Amorphous Semiconductors* (Imperial College Press, London, 1999).
- [3] T. Tiedje *et al.*, *Phys. Rev. Lett.* **46**, 1425 (1981).
- [4] E. Yablonovitch, *Phys. Rev. Lett.* **58**, 2059 (1987); J.D. Joannopolous *et al.*, *Photonic Crystals: Molding the Flow of Light* (Princeton University, Princeton, NJ, 2008).
- [5] C. Jin *et al.*, *Phys. Rev. B* **63**, 195107 (2001); Man *et al.*, *Conference on Lasers and Electro-Optics* (Optical Society of America, San Jose, 2010), paper CThS2.
- [6] M. Florescu, S. Torquato, and P.J. Steinhardt, *Proc. Natl. Acad. Sci. U.S.A.* **106**, 20658 (2009).
- [7] K. Edagawa, S. Kanoko, and M. Notomi, *Phys. Rev. Lett.* **100**, 013901 (2008).
- [8] S. Kivelson and C.D. Gelatt, Jr., *Phys. Rev. B* **19**, 5160 (1979); J. Singh, *J. Non-Cryst. Solids* **299**, 444 (2002).
- [9] F. Lederer *et al.*, *Phys. Rep.* **463**, 1 (2008).
- [10] T. Schwartz *et al.*, *Nature (London)* **446**, 52 (2007).
- [11] H. De Raedt, A. Lagendijk, and P. de Vries, *Phys. Rev. Lett.* **62**, 47 (1989).
- [12] See supplemental material at <http://link.aps.org/supplemental/10.1103/PhysRevLett.106.193904>.
- [13] D. Frenkel and B. Smit, *Understanding Molecular Simulation* (Academic, San Diego, California, 2002).
- [14] A. Szameit *et al.*, *Appl. Phys. B* **82**, 507 (2006).
- [15] N.W. Ashcroft and D.N. Mermin, *Solid State Physics* (Saunders, Fort Worth, Texas, 1976).
- [16] J.M. Ziman, *Models of Disorder: The Theoretical Physics of Homogeneously Disordered Systems* (Alden Press, Oxford, 1979); J.C. Phillips *et al.*, *Nature (London)* **325**, 121 (1987).
- [17] E. Abrahams *et al.*, *Phys. Rev. Lett.* **42**, 673 (1979).
- [18] J. Dong and D.A. Drabold, *Phys. Rev. Lett.* **80**, 1928 (1998); S. John, *Phys. Rev. Lett.* **58**, 2486 (1987).
- [19] J. Robertson, *J. Phys. C* **17**, L349 (1984).
- [20] D. Weaire and D. Hobbs, *Philos. Mag. Lett.* **68**, 265 (1993).
- [21] J.W. Fleischer *et al.*, *Nature (London)* **422**, 147 (2003).